

# $\beta$ decay of the even-even $^{124}\text{Ba}$ nucleus: A test for the interacting boson-fermion-fermion model

---

Brant, Slobodan; Yoshida, N.; Zuffi, L.

Source / Izvornik: **Physical Review C - Nuclear Physics, 2006, 74**

Journal article, Published version

Rad u časopisu, Objavljena verzija rada (izdavačev PDF)

<https://doi.org/10.1103/PhysRevC.74.024303>

Permanent link / Trajna poveznica: <https://um.nsk.hr/um:nbn:hr:217:367993>

Rights / Prava: [In copyright](#) / [Zaštićeno autorskim pravom.](#)

Download date / Datum preuzimanja: **2025-01-01**



Repository / Repozitorij:

[Repository of the Faculty of Science - University of Zagreb](#)



## $\beta$ decay of the even-even $^{124}\text{Ba}$ nucleus: A test for the interacting boson-fermion-fermion model

S. Brant\*

*Department of Physics, Faculty of Science, University of Zagreb, 10000 Zagreb, Croatia*

N. Yoshida†

*Faculty of Informatics, Kansai University, Takatsuki 569-1095, Japan*

L. Zuffi‡

*Dipartimento di Fisica dell'Università di Milano and Istituto Nazionale di Fisica Nucleare, Sezione di Milano Via Celoria 16, Milano 20133, Italy*

(Received 26 May 2006; published 14 August 2006)

The interacting boson-fermion-fermion model approach to  $\beta$  decay is applied to the decay from the even-even  $^{124}\text{Ba}$  to the odd-odd  $^{124}\text{Cs}$  nucleus. The theoretical results for energy levels, electromagnetic properties and  $\beta$  decay rates are compared with experimental data for  $^{124}\text{Cs}$ . The calculated  $\beta$ -decay rates demonstrate that the interacting boson approximation can be applied in the description of  $\beta$  decays from even-even to odd-odd nuclei.

DOI: [10.1103/PhysRevC.74.024303](https://doi.org/10.1103/PhysRevC.74.024303)

PACS number(s): 21.60.Fw, 21.60.Ev, 23.40.-s, 27.60.+j

### I. INTRODUCTION

Theoretical  $\beta$ -decay rates can provide a fine test of nuclear models because they are very sensitive to details of wave functions. In the interacting boson [1] and the interacting boson-fermion model [2] the investigation of  $\beta$  decay has been successfully applied to decays of odd-mass nuclei [3–9]. However,  $\beta$  decay from even-even to odd-odd nuclei in this framework was considered only by the group theory method in the case of spherical nuclei [10].

Models based on the interacting boson approximation have been applied in the description of the structure of vibrational, deformed, and transitional nuclei all over the periodic table. This approach is especially relevant for nuclei in transitional regions, where single-particle excitations and vibrational collectivity are dominant modes. A region of nuclei close to mass number  $A = 130$  is typical for this type of structure. These nuclei are rather soft, and their levels are characterized by a strong mixture of different components. This gives the opportunity to test the model in a more complex situation in respect to the spherical case.

The purpose of this work is twofold. First to study the structure of  $^{124}\text{Cs}$ . Second, and most important, to investigate to what extent the interacting boson approximation can be applied in the description of  $\beta$  decays from even-even to odd-odd nuclei. The present work will be the first numerical study of this type for real nuclei in the interacting boson approximation.

### II. THE IBFFM2 MODEL

#### A. Hamiltonian and energy levels

In the present work we calculate the structure of  $^{124}\text{Cs}$  in the framework of the proton-neutron interacting boson-fermion-fermion model 2 (IBFFM2) [11]. This model is based on the highly successful interacting boson model 2 (IBM2) [12,13] for even-even nuclei, and the interacting boson-fermion model 2 (IBFM2) [2,14,15] for odd- $A$  nuclei. The IBM2/IBFM2/IBFFM2 models are based on the concept of two type of bosons: proton bosons and neutron bosons. We notice that the other model for odd-odd nuclei in the framework of the interacting boson approximation based on one type of bosons, the IBFFM1 [16,17], is very successful in the description of energy levels, electromagnetic properties, and transfer reactions, but due to the fact that it does not distinguish protons and neutrons in the internal structure of bosons, cannot be applied for calculations of  $\beta$  decays.

The advantage of IBFFM2 in respect to IBFFM1 is that IBFFM2 is closer to the microscopic models (as all IBA models based on two type of bosons, i.e., proton bosons and neutron bosons, are in respect to those based on only one type of bosons). However, due to the prohibitively large configuration space, multi- $j$  calculations are far more restricted in IBFFM2 than in IBFFM1. Therefore, some effects caused by configuration mixing that IBFFM1 can take into account, in the IBFFM2 calculations are missing.

In the IBFFM2, an odd-odd nucleus is described as a system consisting of an even-even core, an odd proton and an odd neutron. The basis state of total angular momentum  $I$  is written as

$$|n_{d_\pi} \alpha_\pi L_\pi, n_{d_\nu} \alpha_\nu L_\nu(L), j_\pi j_\nu(J); I\rangle, \quad (1)$$

where  $I = L + J$ ,  $n_{d_\pi}$  ( $n_{d_\nu}$ ), and  $L_\pi$  ( $L_\nu$ ) are the proton (neutron)  $d$ -boson number and the total proton (neutron) boson angular momentum,  $L$  is the total angular momentum of the

\*Electronic address: [brant@sirius.phy.hr](mailto:brant@sirius.phy.hr)†Electronic address: [yoshida@res.kutc.kansai-u.ac.jp](mailto:yoshida@res.kutc.kansai-u.ac.jp)‡Electronic address: [zuffi@mi.infn.it](mailto:zuffi@mi.infn.it)

bosons ( $\mathbf{L} = \mathbf{L}_\pi + \mathbf{L}_\nu$ ),  $j_\pi$  ( $j_\nu$ ) is the angular momentum of the odd proton (neutron), and  $J$  is the total angular momentum of the fermion pairs ( $\mathbf{J} = \mathbf{j}_\pi + \mathbf{j}_\nu$ ). The symbols  $\alpha_\pi$  and  $\alpha_\nu$  are other labels to specify the boson state uniquely. The even-even core is described by the bosons of the IBM2, whereas the odd proton and the odd neutron are independent fermions occupying certain shell-model orbits. The Hamiltonian is

$$H = H^B + H_\pi^F + V_\pi^{\text{BF}} + H_\nu^F + V_\nu^{\text{BF}} + V_{\text{RES}}, \quad (2)$$

where  $H^B$  is the IBM2 Hamiltonian:

$$\begin{aligned} H^B = & \epsilon_d(n_{d_\pi} + n_{d_\nu}) + \kappa(Q_\pi^B \cdot Q_\nu^B) \\ & + \frac{1}{2}\xi_2[(d_\nu^\dagger s_\pi^\dagger - d_\pi^\dagger s_\nu^\dagger) \cdot (\tilde{d}_\nu s_\pi - \tilde{d}_\pi s_\nu)] \\ & + \sum_{K=1,3} \xi_K[(d_\nu^\dagger d_\pi^\dagger)^{(K)} \cdot [\tilde{d}_\pi \tilde{d}_\nu]^{(K)}] \\ & + \frac{1}{2} \sum_{L=0,2,4} c_L^\nu [(d_\nu^\dagger d_\nu^\dagger)^{(L)} \cdot [\tilde{d}_\nu \tilde{d}_\nu]^{(L)}], \end{aligned} \quad (3)$$

with

$$n_{d_\rho} = (d_\rho^\dagger \cdot \tilde{d}_\rho), \quad (4)$$

$$Q_\rho^B = d_\rho^\dagger s_\rho + s_\rho^\dagger \tilde{d}_\rho + \chi_\rho [d_\rho^\dagger \tilde{d}_\rho]^{(2)}. \quad (5)$$

Here  $s_\rho^\dagger$  and  $d_\rho^\dagger$  are the creation operators of the  $s$  boson and the  $d$  boson,  $s_\rho$  is the  $s$ -boson annihilation operator,  $\tilde{d}_\rho$  is the modified  $d$ -boson annihilation operator that is connected to the  $d$ -boson annihilation operator  $d$  by  $\tilde{d}_{\rho m} = (-1)^m d_{-m}$ , where  $\rho = \pi$  ( $\nu$ ) for the proton (neutron) bosons. The Hamiltonian of the odd fermion is given by

$$H_\rho^F = \sum_i \epsilon_{\rho i} n_{\rho i}, \quad (6)$$

where  $n_{\rho i}$  is the number operator of the  $i$ th orbital. For the energy of the  $i$ th orbital, the quasiparticle energy  $\epsilon_{\rho i}$  is taken. The boson-fermion interaction contains the quadrupole, monopole, and exchange interaction:

$$\begin{aligned} V_\rho^{\text{BF}} = & \sum_{i,j} \Gamma_{ij} [(a_i^\dagger \tilde{a}_j]^{(2)} \cdot Q_{\rho'}^B + A \sum n_i n_{d_{\rho'}} + \sum_{i,j} \Lambda_{ki}^j \\ & \times \{ [[d_\rho^\dagger \tilde{a}_j]^{(k)} a_i^\dagger s_\rho]^{(2)} : [s_\rho^\dagger \tilde{d}_{\rho'}]^{(2)} + \text{H.c.} \}, \end{aligned} \quad (7)$$

where  $a_i^\dagger$  represents the fermion creation operator of the  $i$ th orbital and  $\tilde{a}_{im} = (-1)^{i-m} a_{i-m}$ . The symbol  $\rho$  stands for  $\pi$  ( $\nu$ ) for the odd proton (neutron), whereas  $\rho'$  means neutron (proton) if the odd particle is a proton (neutron). The orbital dependence of the quadrupole and the exchange interactions (taken from Ref. [18]) is:

$$\Gamma_{ij} = (u_i u_j - v_i v_j) Q_{ij} \Gamma, \quad (8)$$

$$\Lambda_{ki}^j = -\beta_{ki} \beta_{jk} \left[ \frac{10}{N_\rho (2j_k + 1)} \right]^{1/2} \Lambda, \quad (9)$$

where

$$\beta_{ij} = (u_i v_j + v_i u_j) Q_{ij}, \quad (10)$$

$$Q_{ij} = \langle l_i, \frac{1}{2}; j_i | Y^{(2)} | l_j, \frac{1}{2}; j_j \rangle. \quad (11)$$

Here  $u_j$  ( $v_j$ ) is the unoccupation (occupation) amplitude of the orbit  $j$ . Thus, the strengths of the quadrupole, the monopole,

and the exchange interactions are given by  $\Gamma$ ,  $A$ , and  $\Lambda$ , respectively. The last term on the right-hand side of Eq. (2) is the residual interaction between the odd proton and the odd neutron given by [17]

$$\begin{aligned} V_{\text{RES}} = & 4\pi V_\delta \delta(\mathbf{r}_\pi - \mathbf{r}_\nu) \delta(r_\pi - R_0) \delta(r_\nu - R_0) \\ & - \frac{1}{\sqrt{3}} V_{\sigma\sigma} (\boldsymbol{\sigma}_\pi \cdot \boldsymbol{\sigma}_\nu) + 4\pi V_{\sigma\sigma\delta} (\boldsymbol{\sigma}_\pi \cdot \boldsymbol{\sigma}_\nu) \\ & \times \delta(\mathbf{r}_\pi - \mathbf{r}_\nu) \delta(r_\pi - R_0) \delta(r_\nu - R_0) \\ & + V_T \left[ 3 \frac{(\boldsymbol{\sigma}_\pi \cdot \mathbf{r}_{\pi\nu})(\boldsymbol{\sigma}_\nu \cdot \mathbf{r}_{\pi\nu})}{r_{\pi\nu}^2} - (\boldsymbol{\sigma}_\pi \cdot \boldsymbol{\sigma}_\nu) \right], \end{aligned} \quad (12)$$

where  $\mathbf{r}_{\pi\nu} = \mathbf{r}_\pi - \mathbf{r}_\nu$  and  $R_0$  is the radius of the nucleus.

## B. Electromagnetic transitions

The transition operator consists of the boson and the fermion terms:

$$T = T^B + T^F. \quad (13)$$

More specifically,

$$T^{(E2),B} = e_\pi^B Q_\pi^B + e_\nu^B Q_\nu^B, \quad (14)$$

$$T_\rho^{(E2),F} = \sum_{i,j} e'_{i,j} [a_i^\dagger \tilde{a}_j]^{(2)}, \quad (15)$$

for  $E2$  and

$$T^{(M1),B} = \sqrt{\frac{3}{4\pi}} (g_\pi^B L_\pi^B + g_\nu^B L_\nu^B), \quad (16)$$

$$T_\rho^{(M1),F} = \sum_{i,j} e_{i,j}^{(1)} [a_i^\dagger \tilde{a}_j]^{(1)}, \quad (17)$$

for  $M1$ . The coefficients in the fermion operators above are connected to the effective charges ( $e_\rho^F$ ) and the gyromagnetic factors ( $g_l, g_s$ ) by

$$e'_{i,j} = -\frac{e_\rho^F}{\sqrt{5}} (u_i u_j - v_i v_j) \langle i || r^2 Y^{(2)} || j \rangle, \quad (18)$$

$$e_{i,j}^{(1)} = -\frac{1}{\sqrt{3}} (u_i u_j + v_i v_j) \langle i || g_l \mathbf{l} + g_s \mathbf{s} || j \rangle. \quad (19)$$

## C. $\beta$ decay

In treating the  $\beta$  decay from an even-even nucleus to an odd-odd nucleus, we adopt the same formulation as in Ref. [3], which was originally applied to the  $\beta$  decay from an odd- $A$  to an odd- $A$  nucleus. The IBFFM image of the Fermi  $\sum_k \mathbf{t}^\pm(k)$  and the Gamow-Teller transition operator  $\sum_k t^\pm(k) \sigma(k)$  are written as

$$O^F = \sum_j -\sqrt{2j+1} [P_\pi^{(j)} P_\nu^{(j)}]^{(0)}, \quad (20)$$

$$O^{\text{GT}} = \sum_{j'j} \eta_{j'j} [P_\pi^{(j')} P_\nu^{(j)}]^{(1)}, \quad (21)$$

where

$$\eta_{j'j} = -\frac{1}{\sqrt{3}} \langle l' \frac{1}{2}; j' || \sigma || l \frac{1}{2}; j \rangle = -\delta_{l'l} \sqrt{2(2j'+1)(2j+1)} W(lj' \frac{1}{2} 1; \frac{1}{2} j). \quad (22)$$

The operator  $P_\rho^{(j)}$  stands for the boson-fermion image of the particle transfer operator. For the transitions from an even-even nucleus to an odd-odd, it can be either of the two operators:

$$A_m^{\dagger(j)} = \zeta_j a_{jm}^\dagger + \sum_{j'} \zeta_{jj'} s^\dagger [\tilde{d} a_{j'm}^\dagger]^{(j)} \quad (23a)$$

or

$$\tilde{B}_m^{(j)} = -\theta_j^* s a_{jm}^\dagger - \sum_{j'} \theta_{jj'}^* [\tilde{d} a_{j'm}^\dagger]^{(j)}. \quad (23b)$$

In the case that we study:  $^{124}\text{Ba} \rightarrow ^{124}\text{Cs}$ , the parent nucleus  $^{124}\text{Ba}$  has  $N_\pi = 3$  proton bosons and  $N_\nu = 7$  neutron bosons, whereas the daughter nucleus  $^{124}\text{Cs}$  has  $N_\pi = 2$  proton bosons and  $N_\nu = 6$  neutron bosons. Therefore, both for the proton and the neutron, the transfer operator involves the creation of a fermion and the annihilation of one boson. Thus the operators of Eq. (23b) are applicable:

$$P_\pi^{(j')} = \tilde{B}_\pi^{(j')}, \quad P_\nu^{(j)} = \tilde{B}_\nu^{(j)}. \quad (24)$$

The coefficients  $\theta_j, \theta_{jj'}$  appearing in Eq. (23b) are determined, for the proton and the neutron separately, by the following conditions from Ref. [2]:

$$\theta_j = \frac{v_j}{\sqrt{N}} \frac{1}{K_j''}, \quad (25a)$$

$$\theta_{jj'} = u_j \beta_{j'j} \left( \frac{10}{2j+1} \right)^{1/2} \frac{1}{K_j K_{j'}''}. \quad (25b)$$

Here  $N$  is the number of bosons, and the constants  $K, K_j''$  are determined by

$$K = \left( \sum_{j'j} \beta_{j'j}^2 \right)^{1/2} \quad (26)$$

and

$$\sum_{\alpha J} \langle \text{even}; 0_1^+ || B^{\dagger j} || \text{odd}; \alpha J \rangle^2 = (2j+1) v_j^2. \quad (27)$$

If the odd fermion is a hole,  $u_j$  and  $v_j$  are interchanged in Eqs. (25a)–(27). The squares of the  $\beta$ -decay matrix elements are

$$\langle M_F \rangle^2 = B(F) = \frac{1}{2I_i + 1} |\langle I_f || O^F || I_i \rangle|^2 \quad (28)$$

$$\langle M_{\text{GT}} \rangle^2 = B(\text{GT}) = \frac{1}{2I_i + 1} |\langle I_f || O^{\text{GT}} || I_i \rangle|^2 \quad (29)$$

from which the  $ft$  value is calculated by

$$ft = \frac{6163}{\langle M_F \rangle^2 + (G_A/G_V)^2 \langle M_{\text{GT}} \rangle^2} \quad (30)$$

in units of second, where  $(G_A/G_V)^2 = 1.59$ .

TABLE I. Parameters of the Boson Hamiltonian of  $^{124}\text{Xe}$  ( $N_\nu = 6, N_\pi = 2$ ) and  $^{124}\text{Ba}$  ( $N_\nu = 7, N_\pi = 3$ ). The unit of the energy is MeV except for  $\chi_\rho$  which has no dimension.

Nucleus	$\epsilon$	$\kappa$	$\chi_\pi$	$\chi_\nu$	$c_0^\nu$	$c_2^\nu$	$\xi_1, \xi_2$	$\xi_3$
$^{124}\text{Xe}$	0.70	-0.145	-0.80	0.00	0.05	-0.10	0.24	-0.18
$^{124}\text{Ba}$	0.72	-0.137	-0.90	-0.20	-0.05	-0.12	0.24	-0.18

### III. STRUCTURE OF $^{124}\text{CS}$ IN THE IBFFM2

The interacting boson [1,12,19] and the interacting boson-fermion [2,14,20] (both in versions with one and two type of bosons) and the interacting boson-fermion-fermion model 1 [16,17] have been very successful in the description of nuclear structure in the  $A \approx 130$  region. These very soft nuclei are close to the O(6) limit of the interacting boson model (IBM). The addition of one or two valence fermions can induce strong polarization effects on the boson core, sizeably changing the  $\beta$  deformation and especially the deformation parameter  $\gamma$ . These effects are particularly strong in odd-odd nuclei where both valence protons and neutrons compete in changing the shape of the nucleus. Therefore, the wave functions of odd-odd nuclei in this region can be very complex and are a more sensitive test of the model than those in spherical or rigidly deformed nuclei.

In the IBFFM2 calculation of positive parity states in  $^{124}\text{Cs}$  the core  $^{124}\text{Xe}$  nucleus is described adopting the IBM2 parametrization from Refs. [8,21]. The parameters are shown in Table I.

As the interaction strengths for positive and negative parity states in odd- $A$  nuclei are usually different, in the IBFFM multi- $j$  calculations the average values are used. In Ref. [22] a more consistent procedure was applied. In the IBFFM1 boson-fermion matrix elements involving positive (negative) parity fermion configurations, interaction strengths from the same matrix elements involving positive (negative) parity fermion configurations in the corresponding calculations for odd- $A$  nuclei have been used. In this way levels from odd- $A$  neighbors have been coupled without an additional fitting. At  $\approx 480$  keV in  $^{124}\text{Cs}$ , high-spin states with the  $\pi h_{11/2} \nu h_{11/2}$  configuration start to appear. As our main topic are  $\beta$  transitions, in the present work we limit our attention to low-lying low-spin positive-parity states in  $^{124}\text{Cs}$ . These states are based on positive-parity proton and positive-parity neutron configurations ( $s_{1/2}, d_{3/2}, d_{5/2}, g_{7/2}$ ). The  $\beta$ -decay properties of states based on ( $s_{1/2}, d_{3/2}, d_{5/2}, g_{7/2}$ ) configurations in odd- $A$  neighbors of  $^{124}\text{Cs}$  have been investigated in IBFFM2 in Ref. [8]. Therefore, in avoid calculations in prohibitively large configuration spaces, we consider the parametrizations from Ref. [8] and exclude  $\pi h_{11/2}$  and  $\nu h_{11/2}$  configurations that do not contribute to the structure of low-lying states. In this sense our calculations are similar to the IBFFM1 calculations of Ref. [22].

The single-particle energies for  $^{125}\text{Cs}$  are taken from Ref. [8], whereas those for  $^{123}\text{Xe}$  are taken from Ref. [23], with a slightly bigger gap between the  $h_{11/2}$  and  $s_{1/2}, d_{3/2}$

TABLE II. Single-particle energies (MeV).

Nucleus	$g_{7/2}$	$d_{5/2}$	$s_{1/2}$	$d_{3/2}$	$h_{11/2}$	$h_{9/2}$	$f_{7/2}$
$^{123}\text{Xe}$	-0.20	0.00	1.70	1.75	0.80		
$^{125}\text{Cs}$	0.00	0.05	3.35	3.00	1.50	7.00	8.00

single-particle levels. Their values are shown in Table II. The negative-parity orbits are included only to obtain the quasiparticle energies and the occupation amplitudes. The BCS equations are solved with the gap  $\Delta = 12/\sqrt{A}$  MeV, where  $A$  is the mass number.

Boson-fermion interaction strengths involving odd valence neutrons have to be derived from IBFM2 calculations for  $^{123}\text{Xe}$ . Their mass dependence for  $^{125}\text{Xe}$ ,  $^{127}\text{Xe}$ , and  $^{129}\text{Xe}$  is very smooth [8] and therefore in the present calculation it is assumed that the boson-fermion interaction strengths for  $^{123}\text{Xe}$  and  $^{125}\text{Xe}$  are equal, except for the strength of the exchange interaction that is slightly increased. On the basis of this weak dependence of interaction strengths for odd neutrons on the neutron number, it is reasonable to assume that their values will be conserved in  $^{124}\text{Cs}$ , too. The very smooth mass dependence of boson-fermion interaction strengths for odd- $A$  Xe nuclei was obtained in the IBFM1 calculations, too [23]. The strengths of the boson-fermion interactions are shown in Table III.

For interactions involving odd protons the behavior is different. Boson-fermion interactions in odd-mass Cs nuclei are strongly mass dependent [8]. Calculations in the framework of the core-quasiparticle model for  $^{123}\text{Cs}$  [24] have shown that for this nucleus the strength of the core-particle quadrupole interaction had to be significantly increased in respect to the value used in the same model for neighboring nuclei [25,26]. That increment simulated the effect of core polarization that changes the deformation of the core compared with the deformation of the real neighbouring even-even nuclei. For the sequence of odd- $A$   $^{125,127,129}\text{Cs}$  nuclei the same effect was observed in IBFM2 [8]. The boson-fermion interaction strengths used for the description of these nuclei have been very strong. In the present calculation the interaction strengths for  $^{124}\text{Cs}$  are smaller than in the odd- $A$   $^{125}\text{Cs}$  nucleus [8]. This is especially true for the monopole and exchange interactions, indicating that, due to opposite driving forces of odd protons and odd neutrons, the effective deformations in odd-odd Cs nuclei are smaller than in their odd- $A$  neighboring isotopes. The strengths of the boson-fermion interactions are shown in Table III.

In Ref. [22] the nucleus  $^{124}\text{Cs}$  has been studied by in-beam  $\gamma$ - and  $e^-$ -spectroscopic techniques with the fusion-evaporation reaction  $^{115}\text{In}(^{12}\text{C}, 3n\gamma)$  at 57 MeV. Multipolarities of the main low-energy transitions have been deduced

TABLE III. Boson-fermion interactions (MeV).

Nucleus	$\Gamma$	$A$	$\Delta$
$^{123}\text{Xe}$	0.39	-0.42	0.62
$^{125}\text{Cs}$	0.72	-0.20	0.70

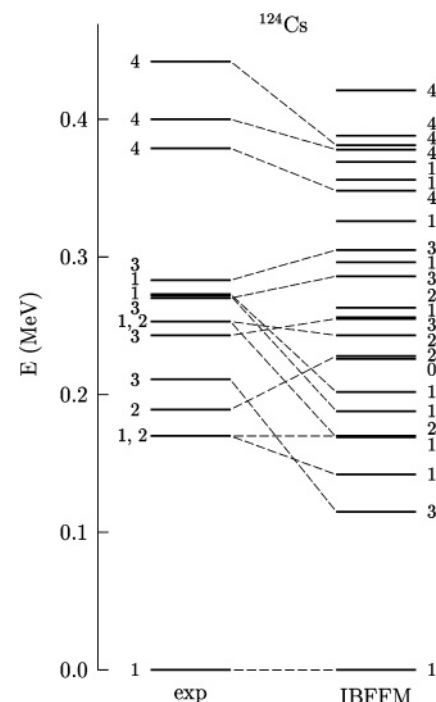
TABLE IV. Proton-neutron interaction (MeV).

$V_\delta$	$V_{\sigma\sigma}$	$V_{\sigma\sigma\delta}$	$V_T$
0	0	0	0.02

from electron spectra. A level scheme was proposed with firm  $I^\pi$  assignments. Several positive-parity states have been previously seen in the  $\beta^+$ /EC radioactive decay of  $^{124}\text{Ba}$  [27]. The  $\gamma$  decay patterns that include the state at 0.170 MeV and a low  $\log_{10} ft$  value indicate that this state is a doublet consisting of the  $1_2^+$  and  $2_1^+$  states. States at 0.253, 0.272, and 0.273 MeV observed in Ref. [27] are assigned as  $1^+$  and their  $\gamma$  decays are compared to the experimental values from Ref. [27].

The residual interaction strengths between the odd proton and the odd neutron are shown in Table IV. In obtaining the energy spectra, we have diagonalized the Hamiltonian (2) matrix for each  $I$ . The dimensions of some matrices exceeded 30000, but no truncation of the basis states has been made. The energy levels are shown in Fig. 1 where the experimental data are taken from Refs. [22,27,28]. The agreement between the experiment and the calculation is very good.

The wave functions of low-lying low-spin positive-parity states, as expected, are very fragmented. Deformation,  $\gamma$  softness, and a relatively small distance between quasiparticle states result, with a strong mixing of fermion configurations. The mixing is stronger than in the IBFM1 calculation [22] and the dominant components show some differences in respect to the predictions of IBFM1. The present calculation is in agreement with the results from Ref. [22], where at low excitation energy the  $\nu d_{3/2}$  configuration had a dominant

FIG. 1. Energy levels in  $^{124}\text{Cs}$ .



role compared to  $\nu s_{1/2}$  and  $\nu d_{5/2}$  configurations. However, proton components of low-lying low-spin positive-parity states in the present calculation are fragmented over all available configurations ( $\pi s_{1/2}, \pi d_{3/2}, \pi d_{5/2}, \pi g_{7/2}$ ), whereas in Ref. [22] the dominant component in the lowest states was  $\pi d_{5/2}$  and above  $\approx 0.250$  MeV excitation energy the  $\pi g_{7/2}$  configuration tended to dominate. For the ground state of  $^{124}\text{Cs}$ , the Nilsson configuration  $1^+(\pi 1/2^+[420]\nu 1/2^+[411])$  with antiparallel angular-momentum coupling ( $K = 0$ ), was considered dominant [27]. The  $\pi 1/2^+[420]$  Nilsson configuration is predominantly based on  $\pi g_{7/2}$  (with large contribution of  $\pi d_{5/2}$ ), whereas the  $\nu 1/2^+[411]$  Nilsson configuration is predominantly based on  $\nu s_{1/2}$ . The wave function of the ground state of  $^{124}\text{Cs}$  in the present calculation is therefore more complex than it would be expected on the basis of the Nilsson scheme.

The electromagnetic transitions are calculated using Eq. (13), with the effective charges  $e_\pi^B = e_\nu^B = 0.15 eb$ ,  $e_\pi^F = 1.5e$ ,  $e_\nu^F = 0.5e$ , and gyromagnetic factors  $g_\pi^B = 0.8\mu_N$ ,  $g_\nu^B = 0\mu_N$ ,  $g_l^\pi = 1\mu_N$ ,  $g_l^\nu = 0\mu_N$ . The spin  $g$ -factor of the odd proton is quenched by a factor 0.85, whereas that of the odd neutron is quenched by 0.5. All effective charges and gyromagnetic factors are equal to those used for the odd- $A$  neighbors [8]. The calculated branching ratios for  $\gamma$  decays are compared to the experimental data in Table V. The main transitions are qualitatively reproduced by the model. Some discrepancies in the decay patterns of  $3^+$  states are due to the existence in a very narrow energy interval, in both theory and experiment, of several  $3^+$  states. These states mix strongly in a way that is not possible to describe in the present calculation. The same problem was encountered in the IBFFM1 calculation [22]. The magnetic and quadrupole moments of the ground state of  $^{124}\text{Cs}$  are known to be  $\mu = +0.673\mu_N$ ,  $Q = -0.74 eb$ . The calculated values  $\mu = +0.91\mu_N$ ,  $Q = -0.43 eb$  are in a fair agreement with the experimental data.

The present calculation is not aimed to describe levels above 0.4 MeV, especially not those with  $I^\pi \geq 5^+$ . It was shown in Ref. [22] that the  $5^+$  level observed at 0.479 MeV and  $6^+$  level at 0.492 MeV have complicated wave functions containing both the  $\pi g_{7/2}\nu g_{7/2}$  and  $\pi h_{11/2}\nu h_{11/2}$  configurations. The higher spin states in the calculation were almost pure  $\pi h_{11/2}\nu h_{11/2}$  states. The structure of wave function of the calculated  $6_2^+$  state supported the existence of the complicated observed decay including bypasses through the  $6^+$  level at 427.6 keV and  $5^+$  level at 373.6 keV [22].

The parent nucleus in the  $\beta$ -decay  $^{124}\text{Ba}$  was analyzed in the IBM2 framework [21]. The Hamiltonian parameters, taken from Ref. [21], are included in Table I. In Table VI the calculated  $\log_{10} ft$  values are compared with the experimental values in  $^{124}\text{Cs}$ . The hierarchy of values for transitions into four lowest  $1^+$  states is reproduced well. The  $\log_{10} ft$  values of the lowest three excited  $1^+$  states are accurately predicted. This nice agreement with experiment gives confidence that the calculation can fairly well describe the  $\beta$  decay to  $^{124}\text{Cs}$ . The discrepancy between theory and experimental data is related to the decay to the ground state, because the strong feeding of the ground state cannot be reproduced.

Due to the fragmentation of wave function components, the  $\beta$ -decay matrix elements consist of many small contributions.

TABLE V. Branching ratios in  $^{124}\text{Cs}$ .

Level (MeV)	Transition	$I_\gamma$ (IBFFM2)	$I_\gamma$ (EXP)
0.170	$1_2^+ \rightarrow 1_1^+$	100	100
0.170	$2_1^+ \rightarrow 1_2^+$	0.0	
	$2_1^+ \rightarrow 1_1^+$	100	100
0.189	$2_2^+ \rightarrow 2_1^+$	0.4	1
	$2_2^+ \rightarrow 1_2^+$	0.1	
	$2_2^+ \rightarrow 1_1^+$	100	100
0.211	$3_1^+ \rightarrow 2_2^+$	0.1	2
	$3_1^+ \rightarrow 2_1^+$	1	
	$3_1^+ \rightarrow 1_2^+$	0.0	
	$3_1^+ \rightarrow 1_1^+$	100	100
0.243	$3_2^+ \rightarrow 3_1^+$	0.0	
	$3_2^+ \rightarrow 2_2^+$	38	100
	$3_2^+ \rightarrow 2_1^+$	95	
	$3_2^+ \rightarrow 1_2^+$	0.1	
	$3_2^+ \rightarrow 1_1^+$	100	27
0.253	$1_3^+ \rightarrow 3_2^+$	0.0	
	$1_3^+ \rightarrow 3_1^+$	0.0	
	$1_3^+ \rightarrow 2_2^+$	33	
	$1_3^+ \rightarrow 2_1^+$	32	
	$1_3^+ \rightarrow 1_2^+$	5	3
	$1_3^+ \rightarrow 1_1^+$	100	100
0.272	$1_4^+ \rightarrow 3_3^+$	0.0	
	$1_4^+ \rightarrow 1_3^+$	0.0	
	$1_4^+ \rightarrow 3_2^+$	0.0	
	$1_4^+ \rightarrow 3_1^+$	0.0	
	$1_4^+ \rightarrow 2_2^+$	3	
	$1_4^+ \rightarrow 2_1^+$	0.0	
	$1_4^+ \rightarrow 1_2^+$	1	8
	$1_4^+ \rightarrow 1_1^+$	100	100
0.379	$4_1^+ \rightarrow 3_3^+$	12	
	$4_1^+ \rightarrow 3_2^+$	19	
	$4_1^+ \rightarrow 3_1^+$	100	100
	$4_1^+ \rightarrow 2_2^+$	1	
	$4_1^+ \rightarrow 2_1^+$	7	
0.400	$4_2^+ \rightarrow 4_1^+$	0.1	
	$4_2^+ \rightarrow 3_3^+$	0.2	
	$4_2^+ \rightarrow 3_2^+$	100	100
	$4_2^+ \rightarrow 3_1^+$	25	
	$4_2^+ \rightarrow 2_2^+$	2	5
	$4_2^+ \rightarrow 2_1^+$	1	

In addition to the odd fermions, the bosons also contribute to the decay, because in the underlying microscopic structure they contain pairs of fermions. Higher-order terms can have sizable contributions, but in many cases positive and negative contributions to the matrix element can almost cancel each other. The calculated matrix element for the decay to the 1st  $1^+$  state is

$$\langle 1_1^+ (^{124}\text{Cs}) || O^{\text{GT}} || 0_1^+ (^{124}\text{Ba}) \rangle = 0.091. \quad (31)$$

If we classify the contributions according to the neutron configurations in  $^{124}\text{Cs}$ , the largest contribution (as expected from the structure of the wave function) comes from the  $\nu d_{3/2}$ , which gives 0.099, where the leading term from Eqs. (21) and (23b)  $\eta_{j'}\theta_{\pi j'}\theta_{\nu j} s_{\pi} s_{\nu} [a_{\pi j'}^\dagger a_{\nu j}^\dagger]^{(1)}$ , for  $\pi d_{5/2} \nu d_{3/2}$ ,

TABLE VI.  $\log_{10} ft$  values for levels in  $^{124}\text{Cs}$ . For comparison, the experimental  $\log_{10} ft$  values for levels in  $^{126}\text{Cs}$  and  $^{128}\text{Cs}$  are presented, too.

Level	$\log_{10} ft(\text{IBFFM2}, ^{124}\text{Cs})$	$\log_{10} ft(\text{EXP}, ^{124}\text{Cs})$	$\log_{10} ft(\text{EXP}, ^{126}\text{Cs})$	$\log_{10} ft(\text{EXP}, ^{128}\text{Cs})$
$1_1^+$	5.68	4.68(5)	5.36(9)	5.28(5)
$1_2^+$	5.70	5.37(7)	6.36(12)	5.09(13)
$1_3^+$	6.20	6.00(9)	5.49(5)	5.6(5)
$1_4^+$	6.59	6.29(8)	6.44(17)	

contributes 0.087. Contributions arising from  $\nu g_{7/2}$  and  $\nu d_{5/2}$  almost cancel with contributions from  $\nu s_{1/2}$ .

It is interesting to compare the IBFFM2 results with experimental data for  $^{126}\text{Cs}$  and  $^{128}\text{Cs}$ . The calculated  $\log_{10} ft$  value for the ground state of  $^{124}\text{Cs}$  is close to experimental  $\log_{10} ft$  values in  $^{126}\text{Cs}$  and  $^{128}\text{Cs}$ . On the basis of data for static moments of the  $1^+$  ground states in  $^{124,126,128}\text{Cs}$  ( $\mu = +0.673(3), +0.777(4), 0.974(5)\mu_N$ ;  $Q = -0.74(3), -0.68(2), -0.570(8)\text{eb}$ ), it is evident that the ground states of  $^{124,126,128}\text{Cs}$  have very similar wave functions. The structure of ground states of parent Ba nuclei is also very similar. Therefore, the  $\log_{10} ft$  values for ground states of  $^{124,126,128}\text{Cs}$  should be similar, too. The rather low  $\log_{10} ft$  in  $^{124}\text{Cs}$  is an indication of additional correlations, either in the parent or daughter nucleus, on which the  $\beta$ -decay operators are very sensitive.

In constructing the IBFFM image of the  $\beta$ -decay operators, we have adopted the method in which we replace the fermion transfer operators by their IBFFM images and then couple them to construct the  $\beta$ -decay operator [3]. This procedure gives a good approximation as long as the shell-model space and the IBFFM space have good correspondence. In fact, the matrix element of a one-body operator  $c_j^\dagger c_j$  between two states  $|A\rangle$  and  $|B\rangle$  is calculated as

$$\langle B|c_j^\dagger c_j|A\rangle = \sum_C \langle B|c_j^\dagger|C\rangle \langle C|c_j|A\rangle. \quad (32a)$$

The corresponding matrix element in the IBFFM is

$$\langle B'|P_j P_j|A'\rangle = \sum_{C'} \langle B'|P_j|C'\rangle \langle C'|P_j|A'\rangle. \quad (32b)$$

The image  $P_j$  is constructed so that  $c_j$  is well simulated in the so-called  $SD$  plus one-particle space [29], i.e., in the space where one fermion is coupled to the  $SD$  subspace [13,18]. The sum in Eq. (32a), however, includes a part that is outside the subspace:

$$\sum_C = \sum_{C \in SD + \text{one-particle space}} + \sum_{C \notin SD + \text{one-particle space}}. \quad (33)$$

The former sum on the right-hand side is well approximated by coupled transfer operators. But the latter sum is not taken into account in constructing the images of the transfer operators. Thus, if the contribution from the latter sum is large, then appreciable effect will arise. Similar problem arises in the summation in Eq. (32b) because spurious states may be contained. Thus, these combined transfer operators do not necessarily become the proper images when the dimensions of the space become large. For a more precise approximation

it will be desirable to construct the one-body operator by comparing the matrices between the one-body operators directly:

$$\langle B|c_j^\dagger c_j|A\rangle \equiv \langle B|P_j P_j|A\rangle \quad (34)$$

among important states  $|A\rangle, |B\rangle, \dots$  [6], such as the OAI mapping [13] for the microscopic basis of IBM, and its extension to IBFM [29]. The effect from the core excitation can also be appreciable. These effects should be investigated in future study.

The reliable assignment of higher calculated  $1^+$  states to some of the observed levels [27] is not possible. Due to the high density of states at higher excitation energy, the compositions of wave functions depend on details of parametrization of interaction strengths. Accidentally, the theoretical  $\beta$ -decay strength can be concentrated on one or two states at higher excitation energy. In this case the calculated  $\log_{10} ft$  has no direct physical meaning. In the real nucleus the decay strength could be distributed over several states. Nevertheless, the appearance of more than one strongly populated state at higher excitation energy can point to the limitations of the model or to a real physical effect. In the present calculation some calculated  $1^+$  states in three regions of excitation energy have  $\log_{10} ft$  values close or lower than 5.

The first group of strongly populated calculated states appear between 0.35 and 0.5 MeV of excitation energy, i.e., at excitation energy where admixtures of components of the intruder proton  $\pi 9/2^+[404]$  Nilsson configuration are expected in wave functions. As this components are small in the wave function of the ground state of the parent nucleus, they would strongly reduce the transition matrix elements and the theoretical  $\log_{10} ft$  values would be sizable higher. The long half-life ( $T_{1/2} = 6.3s$ ) of the  $7^+$  isomer at 462.8 keV in  $^{124}\text{Cs}$  suggests the presence of the  $\pi 9/2^+[404]$  intruder [22]. In light odd- $A$  Sb, I, and Cs nuclei, a pronounced prolate minimum associated with the  $\pi 9/2^+[404]$  orbital occurs dramatically low in excitation energy. It is formed by particle-hole excitations across the closed shell ([30] and references therein). A proton is excited from the lower shell leaving a hole in  $\pi g_{9/2}$  and appearing as a valence  $\pi g_{7/2}$  or  $\pi d_{5/2}$  particle. The intruder configuration is of the one-hole ( $\pi g_{9/2}$ )-two particle (a pair of protons in  $\pi g_{7/2}$  or  $\pi d_{5/2}$ ) type. The coupling with  $\pi g_{9/2}$  is very strong, pushing this configuration strongly down, and the pairing of two protons in  $\pi g_{7/2}$  or  $\pi d_{5/2}$  additionally decreases the excitation energy. The corresponding states in  $^{124}\text{Cs}$  would therefore be based on four-quasiparticles. In the IBFFM2 picture the decay would occur between states that have very different boson structure,

both in deformation and in the fermion composition of the bosons, resulting in a big quenching of the, otherwise strong,  $\pi g_{9/2} \rightarrow \nu g_{7/2}$  transition. In the proton-neutron quasiparticle random-phase approximation (pnQRPA) the “particle-hole” interaction does not cause significant quenchedings of transition matrix elements, whereas the “particle-particle” interaction causes huge quenchedings and in limiting cases even total forbiddenness of decays [31–34]. In the present calculation the valence protons (particles) interact predominantly with neutron bosons (holes) and valence neutrons (holes) interact predominantly with proton bosons (particles). The main part of the interaction (in pnQRPA terms) is the particle-hole interaction. The predominant part of the interaction involving  $\pi g_{9/2}$  would be between protons (holes) and neutron bosons (holes), i.e., of the particle-particle type, which would lead to strong quenchedings of transitions to states with admixtures of  $\pi g_{9/2}$  components. The IBM-based model for odd-odd nuclei that includes four-quasiparticle states has not been developed. In relation to the previous discussion [Eqs. (32a), (32b), (33), and (34)], strongly populated calculated states appearing between 0.35 and 0.5 MeV of excitation energy could be the evidence that for these states the shell-model space and the IBFFM space do correspond well.

A state at 800 keV and two around 900 keV, with  $\log_{10} ft$  lower than 5, are predicted in the present calculation. Although this could be an accidental concentration of calculated  $\beta$ -decay strength in three states, we notice that in this mass region states with low  $\log_{10} ft$  values at these excitation energies, have been observed in  $^{132}\text{Pr}$  [35] ( $\log_{10} ft = 4.51$  for the state at 715 keV and  $\log_{10} ft = 4.84$  for the state at 981 keV). The state at 715 keV in  $^{132}\text{Pr}$  has the  $\log_{10} ft$  value that is even smaller than the  $\log_{10} ft$  for the  $1_1^+$  state.

In  $^{124}\text{Cs}$  a group of four rather strongly populated levels is observed between 1.2 and 1.4 MeV of excitation energy [27]. The same group of levels in  $^{126}\text{Cs}$  is observed between 1.2 and 1.3 MeV with the lowest  $\log_{10} ft = 4.54$ . The present IBFFM2 calculation predicts states with  $\log_{10} ft$  values of this order at excitation energies between 1.0 and 1.15 MeV, in fair agreement with experimental data.

The influence of  $\pi h_{11/2}\nu h_{11/2}$  components (that are not included in the present calculation) is difficult to predict. They would admix to wave functions of  $1_1^+$  states, based on  $s_{1/2}$ ,  $d_{3/2}$ ,  $d_{5/2}$ ,  $g_{7/2}$  configurations, through odd- $l$  terms of the

residual proton-neutron interaction. At low excitation energies  $\pi h_{11/2}\nu h_{11/2}$  components are not present. At high excitation energies, where the level density is high, their percentage in wave functions of individual calculated states would be accidental.

The  $F$ -spin vector boson components [1] are contained in very high  $1^+$  levels. But as far as low-lying states and even states up to 1.5 MeV are concerned, the effect is very small because the excitation energy ( $\approx 2.5$  MeV) of the first  $1^+$  level in the core nucleus  $^{124}\text{Xe}$  is high.

#### IV. CONCLUSION

The structure of  $^{124}\text{Cs}$  has been investigated in the framework of the interacting boson-fermion-fermion model. A detailed analysis, that included the calculation of the spectra and electromagnetic transitions has been performed. The IBFFM2 images of the Fermi and Gamow-Teller transition operators do not contain any free parameter. In contrast to shell model calculations of  $\log_{10} ft$  values, where additional normalization is used, the  $\log_{10} ft$  values in IBFFM2 are obtained in a parameter free calculation, without any additional normalization. The  $\log_{10} ft$  values depend only on the wave functions of parent and daughter nuclei. The calculated  $\beta$ -decay rates have demonstrated that the IBFFM2 wave functions of the parent and daughter nuclei are realistic and that the interacting boson approximation can be applied in the description of  $\beta$  decays from even-even to odd-odd nuclei. The limitation of this approach is given by the accuracy in approximating fermion pairs with bosons, and simulating the  $\beta$ -decay operators with operators in the  $SD$  plus one-particle space. For majority of levels the correspondence between the shell-model space and the IBFFM space is good, resulting in good agreement between experimental data and theoretical results.

#### ACKNOWLEDGMENTS

N. Yoshida is thankful to the financial support by “Academic Frontier” Project and Organization for Research and Development of Innovative Science and Technology (ORDIST) of Kansai University.

[1] F. Iachello and A. Arima, *The Interacting Boson Model* (Cambridge University Press, Cambridge, 1987).  
 [2] F. Iachello and P. Van Isacker, *The Interacting Boson-Fermion Model* (Cambridge University Press, Cambridge, 1991).  
 [3] F. Dellagiocoma, Ph.D. thesis, Yale University, 1988; F. Dellagiocoma and F. Iachello, *Phys. Lett.* **B218**, 299 (1989).  
 [4] G. Maino and L. Zuffi, in *Proceedings of the 7th International Conference on Nuclear Reaction Mechanisms, Varenna, 1994*, edited by E. Gadioli (University of Milan, Milan, 1994), p. 765.  
 [5] G. Maino, in *Proceeding of the International Symposium on Perspectives for the Interacting Boson Model, Padova, 1994*, edited by R. F. Casten, A. Vitturi, A. B. Balantekin, B. R. Barrett,

J. N. Ginocchio, G. Maino, and T. Otsuka (World Scientific, Singapore, 1995), p. 617.  
 [6] N. Yoshida, L. Zuffi, and A. Arima, *Czech. J. Phys.* **52**, C615 (2002).  
 [7] N. Yoshida, L. Zuffi, and S. Brant, *Phys. Rev. C* **66**, 014306 (2002).  
 [8] L. Zuffi, S. Brant, and N. Yoshida, *Phys. Rev. C* **68**, 034308 (2003).  
 [9] S. Brant, N. Yoshida, and L. Zuffi, *Phys. Rev. C* **70**, 054301 (2004).  
 [10] G. Maino and L. Zuffi, in *Proceedings of the 5th International Spring Seminar on Nuclear Physics, Ravello, 1996*, edited by A. Covello (World Scientific, Singapore, 1996), p. 611.



- [11] N. Yoshida, H. Sagawa, and T. Otsuka, Nucl. Phys. **A567**, 17 (1994).
- [12] A. Arima, T. Otsuka, F. Iachello, and I. Talmi, Phys. Lett. **B66**, 205 (1977).
- [13] T. Otsuka, A. Arima, and F. Iachello, Nucl. Phys. **A309**, 1 (1978).
- [14] J. Panqueva, H. P. Hellmeister, L. Lühmann, F. J. Bergmeister, K. P. Lieb, and T. Otsuka, Nucl. Phys. **A389**, 424 (1982).
- [15] C. E. Alonso, J. M. Arias, R. Bijker, and F. Iachello, Phys. Lett. **B144**, 141 (1984).
- [16] V. Paar, *Capture Gamma-Ray Spectroscopy and Related Topics-1984*, edited by S. Raman, AIP Conf. Proc. No. 125 (AIP, New York, 1985), p. 70; S. Brant, V. Paar, and D. Vretenar, Z. Phys. A **319**, 355 (1984); V. Paar, D. K. Sunko, and D. Vretenar, *ibid.* **327**, 291 (1987).
- [17] S. Brant and V. Paar, Z. Phys. A **329**, 151 (1988).
- [18] O. Scholten, Ph.D. thesis, University of Groningen, 1980.
- [19] A. Arima and F. Iachello, Phys. Rev. Lett. **35**, 1069 (1975); Ann. Phys. (NY) **99**, 253 (1976); **111**, 201 (1978); **123**, 468 (1979).
- [20] F. Iachello and O. Scholten, Phys. Rev. Lett. **43**, 679 (1979).
- [21] G. Puddu, O. Scholten, and T. Otsuka, Nucl. Phys. **A348**, 109 (1980).
- [22] A. Gizon, J. Timár, J. Gizon, B. Weiss, D. Barnéoud, C. Foin, J. Genevey, F. Hannachi, C. F. Liang, A. Lopez-Martens, P. Paris, B. M. Nyakó, L. Zolnai, J. C. Merdinger, S. Brant, and V. Paar, Nucl. Phys. **A694**, 63 (2001).
- [23] Gh. Cata-Danil, D. Bucurescu, A. Gizon, and J. Gizon, J. Phys. G **20**, 1051 (1994).
- [24] A. Gizon, B. Weiss, P. Paris, C. F. Liang, J. Genevey, J. Gizon, V. Barch, Gh. Cata-Danil, J. S. Dionisio, J. M. Lagrange, M. Pautrat, J. Vanhorenbeeck, Ch. Vieu, L. Zolnai, J. M. Arias, J. Barea, and Ch. Droste, Eur. Phys. J. A **8**, 41 (2000).
- [25] K. Starosta, Ch. Droste, T. Morek, J. Srebrny, D. B. Fossan, D. R. LaFosse, H. Schnare, I. Thorslund, P. Vaska, M. P. Waring, W. Satula, S. G. Rohoziski, R. Wyss, I. M. Hibbert, R. Wadsworth, K. Hauschild, C. W. Beausang, S. A. Forbes, P. J. Nolan, and E. S. Paul, Phys. Rev. C **53**, 137 (1996).
- [26] T. Morek, K. Starosta, Ch. Droste, D. Fossan, G. Lane, J. Sears, J. Smith, and P. Vaska, Eur. Phys. J. A **3**, 99 (1998).
- [27] B. Weiss, A. Gizon, C. F. Liang, P. Paris, and the Isocele Collaboration, Z. Phys. A **323**, 227 (1986).
- [28] H. Iimura, J. Katanaka, K. Kitao, and T. Tamura, Nucl. Data Sheets **80**, 895 (1997).
- [29] N. Yoshinaga, Y. D. Devi, and A. Arima, Phys. Rev. C **62**, 024309 (2000).
- [30] K. Heyde, P. Van Isacker, M. Waroquier, J. L. Wood, and R. A. Meyer, Phys. Rep. **102**, 291 (1983).
- [31] P. Vogel and M. R. Zirnbauer, Phys. Rev. Lett. **57**, 3148 (1986).
- [32] O. Civitarese, A. Faessler, and T. Tomoda, Phys. Lett. **B194**, 11 (1987).
- [33] J. Suhonen, T. Taigel, and A. Faessler, Nucl. Phys. **A486**, 91 (1988).
- [34] J. Suhonen, A. Faessler, T. Taigel, and T. Tomoda, Phys. Lett. **B202**, 174 (1988).
- [35] D. Bucurescu, D. Barnéoud, Gh. Căta-Danil, T. von Egidy, J. Genevey, A. Gizon, J. Gizon, C. F. Liang, P. Paris, B. Weiss, S. Brant, V. Paar, and R. Pezer, Nucl. Phys. **A587**, 475 (1995).